J. Membrane Biol. 194, 33–45 (2003)
DOI: 10.1007/s00232-003-2023-y

The Journal of
Membrane
Biology

External Ni^{2+} and ENaC in A6 Cells: Na^+ Current Stimulation by Competition at a Binding Site for Amiloride and Na^+

D. Cucu[1], **J. Simaels**[1], W. Van Driessche[1], W. Zeiske[2]
[1]Laboratory of Physiology, K. U. Leuven, Campus Gasthuisberg O/N, B-3000 LEUVEN, Belgium
[2]Institut für Zoophysiologie, Universität Osnabrück, Barbarastrasse, 11, D-49069 Osnabrück, Germany

Received: 15 January 2003

Abstract. In cultured A6 monolayers from distal *Xenopus* kidney, external Ni^{2+} stimulated active Na^+ uptake via the epithelial Na^+ channel, ENaC. Transepithelial capacitance measurements ruled out exocytosis of ENaC-containing vesicles underlying the Ni^{2+} effect. Na^+ current noise analysis was performed using the neutral Na^+-channel blocker 6-chloro-3,5-diamino-pyrazine-2-carboxamide (CDPC) and amiloride. The analysis of CDPC-induced noise in terms of a three-state channel model revealed that Ni^{2+} elicits an increase in the number of open channels as well as in the spontaneous open probability. While Ni^{2+} had no influence on CDPC-blocker kinetics, the macroscopic and microscopic blocking kinetics of amiloride were affected. Ni^{2+} turned out to compete with amiloride for a putative binding site but not with CDPC. Moreover, external Na^+—known to compete with amiloride and so producing the "self-inhibition" phenomenon—and Ni^{2+} exerted mutually exclusive analogous effects on amiloride kinetics. Na^+ current kinetics revealed that Ni^{2+} prevents ENaC to be downregulated by self-inhibition. Co^{2+} behaved similarly to Ni^{2+}, whereas Zn^{2+} did not. Attempts to disclose the chemical nature of the site reacting with Ni^{2+} suggested cysteine but not histidine as reaction partner.

Key words: Ni^{2+} — ENaC — A6 cells — Self-inhibition — Noise analysis

Correspondence to: W. Van Driessche; email: Willy.VanDriessche@med.KULeuven.ac.be

Introduction

The epithelial Na^+ channel (ENaC) is a member of the newly identified channel family ENaC/degenerin. Studies of the membrane topology describe the channel as a multimer made of the homologous α-, β- and γ-subunits, each of which being formed by two transmembrane segments (M1 and M2) separated by a large extracellular domain. The extracellular loop represents more than 50% of each subunit protein and it is not found in other channel families (Benos & Stanton, 1999). It is thought to characterize the ENaC/degenerin family and contains two highly conserved cysteine rich domains (CRD). The fact that so much of the primary structure of ENaC lies in the extracellular domain was taken as a hint for the extracellular localization of some well-known "regulatory" sites as well as of an amiloride-binding site in this segment. Amiloride has been shown to be the specific label of choice for ENaC. Besides a specific binding site localized in the pre-M2 segments of each ENaC subunit (Schild et al., 1997), Ismailov et al. (1997) identified a six-amino-acid residue track in the extracellular loop of α-ENaC as a second specific binding site.

Many regulatory mechanisms modulate the activity of ENaC. For instance, the extracellular Na^+ concentration has a marked effect on Na^+ transport described by two phenomena (Lindemann, 1984): feedback inhibition (related to a rise of intracellular Na^+ concentration after increasing external Na^+) and self-inhibition (caused solely by external Na^+). Apart from regulation by hormones, which is typical of Na^+ transport in frog skin, kidney, urinary bladder or colon, Na^+ uptake via ENaC is sometimes stimulated by a number of polyvalent cations. Several decades ago, Hillyard (Hillyard & Gonick, 1976) suggested direct interaction of external Cd^{2+} ions with the frog skin Na^+ channel. In the isolated uri-

nary bladder of the toad *Bufo marinus,* a clear stimulation of Na^+ transport was reported after addition of external Mg^{2+} (Aguilera, Kirk & DiBona, 1978). Furthermore, it turned out that mercurial organic compounds and polyvalent inorganic cations such as La^{3+}, Zn^{2+}, Cd^{2+} and Ni^{2+} are able to increase Na^+ uptake in frog skin (Zeiske, 1979). These ions were studied in relation to the process of Na^+ self-inhibition, with which they were interfering. For the apical membrane of frog skin Grinstein et al. (Grinstein, Candia & Erlij, 1978) related the action of di- and trivalent cations to surface charge screening. Li and Lindemann (1980) only briefly remarked that Ni^{2+} stimulates Na^+ transport in frog skin, without a detailed study or interpretation. Recently, the influence of Ni^{2+} on rat ENaC and mouse ENaC has been described in studies on ENaC-expressing oocytes (Segal et al., 2002; Sheng, Perry & Kleyman, 2002). In both studies, the authors report a noticeable inhibition of the amiloride-sensitive Na^+ current when Ni^{2+} was added from the extracellular side, thus the opposite of Ni^{2+} action on amphibian ENaC.

Ni^{2+} is a transition metal whose reactivity depends on the coordination geometry or its oxidation state. Although Ni^{2+} is able to catalyze, in trace amounts, metabolic reactions by binding to metalloenzymes, its accumulation from the environment represents a serious risk for human health (Watt & Ludden, 1999). Among the known harmful effects of Ni^{2+} are skin allergies, lung fibrosis, kidney and cardiovascular system poisoning and stimulation of neoplastic transformation (Denkhaus & Salnikow, 2002). The experiments reported in the present paper were performed in an effort to investigate the influence of Ni^{2+} on the Na^+ transport in amphibian renal epithelial cells. Using the analysis of transepithelial conductance (G_T), capacitance (C_T), short-circuit current (I_{sc}), I_{sc} kinetics and CDPC/amiloride-induced blocker noise, we can show that Ni^{2+} stimulates Na^+ transport across A6-cell ENaC. Moreover, Ni^{2+} competes with apical Na^+ and amiloride (but not with CDPC) for a putative site resident in the extracellular loop of one or more channel subunits. The thiol reagent, para-chloro-mercuribenzoate (p-CMB) imitated the action of Ni^{2+}, whereas diethyl pyrocarbonate (DEPC), a histidine reagent, could not prevent ENaC stimulation by Ni^{2+}. Extracellular Co^{2+} has an effect comparable to Ni^{2+} although to a lesser degree, while Zn^{2+} is inert.

Materials and Methods

Cell Culture

All experiments were carried out on polarized monolayers of A6 cells (a gift from Dr. J. P. Johnson, University of Pittsburgh, Pittsburgh, PA) grown on permeable Anopore filters (pore size 0.2 μm; Nunc Intermed, Roskilde, Denmark) at 28°C and 1% CO_2 in a humidified incubator. The growth medium was renewed twice weekly and consisted of a 1:1 mixture of Leibovitz's L-15 and Ham's F-12 media, supplemented with 10% fetal bovine serum (Sigma, St. Louis, MO), 2.6 mM $NaHCO_3$, 3.8 mM glutamine, 95 IU ml^{-1} penicillin and 95 μg ml^{-1} streptomycin.

Solutions and Chemicals

Solutions contained (in mM): 102 NaCl, 2.5 $KHCO_3$, 1 $CaCl_2$ (200 mosmol/kg H_2O, pH = 8.2). In A6 epithelial cells, the apical membrane has negligible water permeability, thus the apical osmolality does not influence Na^+ current or conductance (De Smet, Simaels & Van Driessche, 1995). Solutions with different NaCl concentrations such as 30, 60 and 90 mM were therefore prepared by diluting NaCl Ringer with NaCl-free saline. In HEPES-buffered solutions (pH = 7.6), Ni^{2+} was a weaker current stimulator. Possibly Ni^{2+} forms mixed complexes, thus reducing the free Ni^{2+} concentration, or else the Ni^{2+} effect may be pH sensitive. To avoid putative formation of Ni^{2+} complexes we decided to perform experiments in $KHCO_3$-buffered solutions at pH = 8.2. This pH remains stable after Ni^{2+} addition. Solutions containing para-chloro-mercuribenzoate (p-CMB) and the histidine reagent diethyl pyrocarbonate (DEPC) were freshly prepared before use. All chemicals were purchased from Merck (Darmstadt, Germany), except for the amiloride, p-CMB and DEPC, which were obtained from Sigma (St. Louis, MO) and CDPC, which was purchased from Aldrich (Milwaukee, WI).

Electrophysiological Measurements

Current and voltage electrodes for the Ussing-type chamber (De Wolf & Van Driessche, 1986) were made of Ag-AgCl wires and connected to the solutions with 1 M KCl agar bridges. The monolayers were short-circuited with a high-speed voltage clamp. The transepithelial conductance (G_T) was measured by imposing a 1 Hz sine wave of 5 mV amplitude to the tissue. Na^+ transport (I_{Na}) was defined as the amiloride-sensitive component of I_{sc}.

Continuous recording of the transepithelial capacitance (C_T), which is a convenient measure of membrane area, was based on the current elicited by five 5-mV sine waves of 2, 2.7, 4.1, 5.4 and 8.2 kHz, respectively, across the monolayer, as described previously (Van Driessche et al., 1999). Model calculations based on a lumped, two-membrane model demonstrated that in the high-frequency range C_T equals the equivalent capacitance of the series arrangement of the apical (C_{ap}) and basolateral capacitance (C_{bl}) (Van Driessche et al., 1999):

$$\frac{1}{C_T} = \frac{1}{C_{ap}} + \frac{1}{C_{bl}} \quad (1)$$

As, in A6 tissues, C_{bl} is about 12 times larger than C_{ap}, changes in C_T will reflect mainly area changes of the apical membrane, i.e., the result of endo- and exocytotic processes.

Noise Analysis

For calculation of the kinetic parameters we used two blockers: the highly specific blocker amiloride and a weak, reversible blocker of Na^+ transport CDPC (6-chloro-3,5-diamino-pyrazine-2-carboxamide). For the CDPC-induced noise we used a pulse protocol similar to that described by Blazer-Yost et al. (Blazer-Yost, Liu & Helman, 1998). The apical surface of A6 epithelia was exposed alternatively to 10 or 40 μM CDPC for periods of 5 minutes. Current noise at both blocker concentrations was amplified, digitized and Fourier-transformed to yield power density spectra.

During each 5-min period we recorded noise spectra as the mean of 50 sweeps of 2 s duration, resulting in a fundamental frequency of 0.5 Hz. The amiloride-insensitive current (I_{Ami}) was measured by blocking the channels at the apical side with 50 μM amiloride. The blocker-sensitive, macroscopic current (I_{Na}) was calculated as:

$$I_{Na} = I_{sc} - I_{Ami} \tag{2}$$

The interaction of CDPC with the Na^+ channel induced a Lorentzian component in the power density spectra. The two Lorentzian parameters, the low-frequency plateau (S_o) and the corner frequency (f_c), were determined by non-linear curve fitting of the spectra (Lindemann & Van Driessche, 1977). The on (k_{on}) and off (k_{off}) rates of the blocking reaction were calculated from:

$$2\pi f_c = k_{on}[B] + k_{off} \tag{3}$$

where [*B*] is the blocker concentration. Using the Na^+ currents and the Lorentzian parameters (f_c and S_o) obtained from noise analysis, we estimated the single-channel current (i_{Na}) and the density of open, amiloride-sensitive Na^+ channels in the apical membrane (N_o) according to Helman et al. (Helman & Baxendale, 1990). Then, single-channel currents in the presence of 10 μM CDPC (i_{Na}^{10}) could be used as single-channel currents in the absence of blocker, since both do not differ significantly from each other:

$$i_{Na}^{10} = \frac{S_o^{10}(2\pi f_c^{10})^2}{4I_{Na}^{10}k_{on}[B]} \tag{4}$$

where S_o^{10}, f_c^{10} and I_{Na}^{10} are the values of S_o, f_c and I_{Na} in the presence of 10 μM CDPC. N_o for functional channels at 10 μM CDPC (N_o^{10}) is given by:

$$N_o^{10} = I_{Na}^{10}/i_{Na}^{10} \tag{5}$$

N_o in the absence of CDPC is calculated as follows:

$$N_o = N_o^{10}\left(1 + P_o\frac{[B]}{K_B}\right) \tag{6}$$

where K_B is the equilibrium constant for the blocking reaction of open channels (k_{off}/k_{on}) in μM. P_o represents the open probability of the Na^+ channel for spontaneous blocker independent conductance fluctuation. According to Helman (Helman & Baxendale, 1990), P_o was calculated using K_B from the fractional inhibition of the blocker-sensitive Na^+ transport, $I_{Na}^{40}/I_{Na}^{10}(I_{Na}^{40/10})$ elicited by increasing the CDPC concentration from 10 to 40 μM:

$$P_o = \frac{1 - I_{Na}^{40/10}}{40I_{Na}^{40/10} - 10}K_B \tag{7}$$

The analysis of the amiloride-induced noise was restricted to the evaluation of the blocking/unblocking rate constant according to Eq. 3.

Data Analysis

Linear least-square fitting was used to obtain kinetic parameters (k_{on}, and k_{off}). For all experiments, results are given as means ± SEM; *n* represents the number of experiments.

Results

Effects of NI^{2+} on Na^+ Current (I_{Na}), Transepithelial Conductance (G_T) and Transepithelial Capacitance (C_T)

Figure 1*A* shows the time courses of I_{sc}, G_T and C_T for a typical experiment from a series of 6, after addition of 2 mM $NiCl_2$ to the apical Ringer solution ($n = 6$). As a result, I_{sc} rose rapidly by roughly 50%, followed by a 15% decline to a plateau, which was reached in few minutes. The steady state is, however, much above the control value of I_{sc}. The Ni^{2+}-induced increase of current goes along with an increase of conductance (G_T). The initial phase of current stimulation can be described by a single exponential with a time constant of 0.5 ± 0.02 min (*not shown*). After Ni^{2+} removal, a rapid return (0.41 ± 0.04 min) of I_{sc} to the initial value was noticed, indicating a perfect reversibility of the process. The evidence that the Ni^{2+}-stimulated current is a Na^+ current comes from the fact that 100 μM amiloride inhibits all of the current (*data not shown*). Moreover, 2 mM Ni^{2+} added to Na^+-free solutions had no effect on either current, which is close to zero, or conductance (*data not shown*). The fast onset of Na^+-transport activation and the rapid washout suggest a site of action of Ni^{2+} at the extracellular surface of A6 cells.

The dose-response curve depicted in Fig. 1*B* suggests saturation behavior of the Ni^{2+}-induced I_{Na} stimulation (current peaks). The half-maximal effect was reached at a Ni^{2+} concentration (K_m) of 0.10 ± 0.02 mM, whereas 2 mM Ni^{2+} were sufficient for the complete stimulation of the current. The I_{Na} stimulation may be due to changes of basolateral Na/K-ATPase activity or changes of the apical Na^+ transport mechanism. However, since the effect of Ni^{2+} is very rapid and shows an equally fast reversibility, stimulation of the usually rate-limiting apical Na^+ transfer step seems more likely. Therefore, Ni^{2+} probably stimulates transport through the epithelial Na^+ channel (ENaC). Several studies on tight epithelia suggested that apical activation of Na^+ transport might occur by exocytotic insertion of new channels in the apical membrane. Such a process will cause a notable increase in membrane area and therefore in transepithelial capacitance (C_T), which largely reflects the apical membrane area (Jans et al., 2000). Such a relation between I_{Na} and C_T was established for the hormonal activation of apical Na^+ uptake (Van Driessche & Erlij, 1991; Erlij, De Smet & Van Driessche, 1994). As shown in Fig. 1*A*, C_T does not change when Ni^{2+} is added to the apical solution, so the stimulation of apical Na^+ transfer is not related to the insertion of new channels in the apical membrane. Rather, the increase of Na^+ current is most probably the consequence of the activation of the Na^+ transfer through preexistent Na^+ channels in the apical membrane.

Results from CDPC Noise of I_{Na}

To further elucidate the process, it was necessary to examine the parameters that describe the transapical Na^+ current, which is given by:

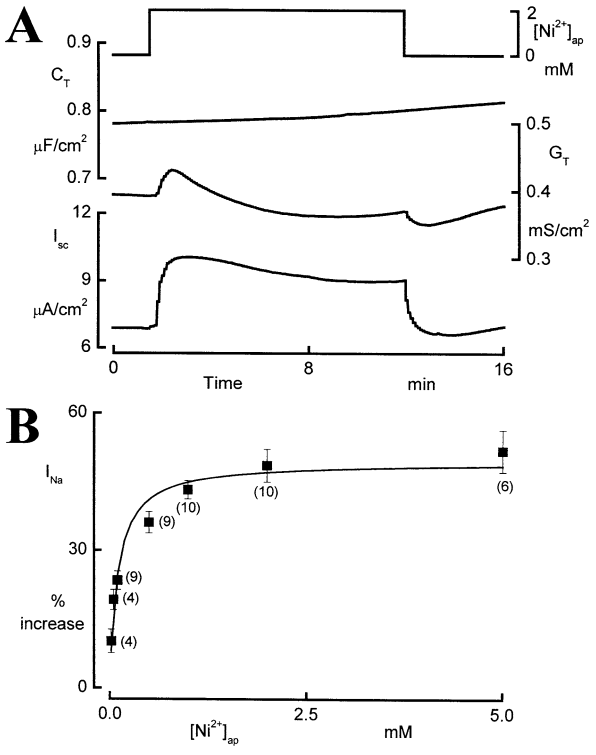

Fig. 1. Effect of Ni^{2+} on the macroscopic transport parameters. (*A*) Effect of 2 mM Ni^{2+} on I_{Na}, G_T and C_T. The apical and basolateral solutions had the same composition (*see* Materials and Methods), where 2 mM Ni^{2+} was added only to apical solution. (*B*) Dose-response relationship for Ni^{2+}-stimulated current. The percentage current increase by Ni^{2+} is plotted as a function of apical Ni^{2+} concentration. A Michaelis-Menten fit of the data gives a K_m of 0.1 ± 0.02 mM and a maximal increase in current by 49.5 ± 2.2%; data are plotted as averages ± SEM. The number of experiments is indicated in parentheses.

$$I_{Na} = i_{Na} N_T = i_{Na} P_o N_o \quad (8)$$

where i_{Na} is the single-channel current, N_o the open-channel density, N_T total number of channels in the apical membrane and P_o open probability. Both N_T and/or P_o can be responsible for changes in apical Na^+ uptake. The determination of i_{Na} and N_o was done by noise analysis. CDPC-induced noise (for details, *see* section Materials and Methods) is easily measurable under conditions of minimal inhibition of Na^+ current. This inhibitor permits the analysis of the blocker dependence of the parameters i_{Na} and N_o much below half-maximal blocker concentration. We used a three-state model (closed ⇆ open ⇆ blocked) to calculate i_{Na} and N_o (Helman & Baxendale, 1990). Because $2\pi f_c$ increased linearly with the CDPC concentration (Fig. 2) we can calculate the k_{on} rate constant (the slope) as 7.4 ± 0.3 $\mu M^{-1}s^{-1}$ and the unblocking rate constant k_{off} = 236.6 ± 14.3 s^{-1} from the ordinate intercept (*see* Materials and Methods). In the presence of 2 mM Ni^{2+}, k_{on} = 8.7 ± 0.6 $\mu M^{-1}s^{-1}$ and k_{off} = 264.7 ± 18.3 s^{-1}. In this

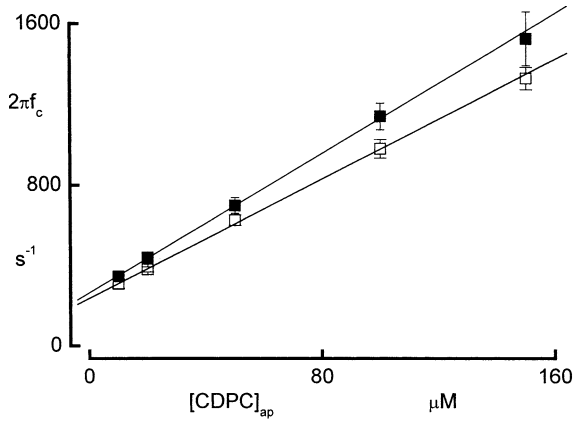

Fig. 2. Effect of Ni^{2+} on the CDPC rate constants of blocker-receptor interaction. Relationship between corner frequency ($2\pi f_c$) and blocker concentration ($[CDPC]_{ap}$) in control conditions (*white symbols*) and when 2 mM Ni^{2+} were added to the apical solution (*black symbols*). Solid lines were obtained by linear regression analysis. Statistical comparison indicates no significant differences between the two conditions. The data represent the mean ± SEM of 5 experiments.

set of 5 experiments, the differences between k_{on} and k_{off} in control and in the presence of Ni^{2+}, respectively, were statistically not significant, showing that the chemical rates ($2\pi f_c$) of the blocker CDPC are not affected by the presence of Ni^{2+}. Figure 3 shows the percentage differences of the ENaC kinetic parameters i_{Na}, N_o and P_o, as revealed by CDPC-induced noise, for the presence of Ni^{2+} relative to control conditions. When 2 mM Ni^{2+} were present in the apical Ringer solution I_{Na} increased, while i_{Na} did not change significantly. Since I_{Na} increase must reflect the changes of i_{Na} and/or N_o the Ni^{2+}-stimulated current reflects an augmentation of N_o, which increased from 18.9 ± 1.5 to 32.9 ± 2.7 million channels/cm^2 by the action of Ni^{2+}. We could also estimate a similar increase of P_o for every experiment in the series of 5.

Interactions between Ni^{2+} and Amiloride

As known since a long time, the epithelial sodium channel is also reversibly blocked by amiloride (Garty & Benos, 1988). The amiloride molecule has a pyrazine ring, as does CDPC, but contains a guanidinium moiety, which is attached to the carboxy-side chain and is charged at pH ≤ 8.7. Some studies suggest that the charged guanidinium group blocks the entrance of the channel directly, while the pyrazine ring binds to a second site in the ENaC protein (McNicholas & Canessa, 1997). However, both parts of the molecule are necessary for maximal inhibition of Na^+ transport (Li, Cragoe & Lindemann, 1985). Figure 4*A* shows the percentage inhibition of Na^+ current by increasing concentrations of apical amiloride in control and in solutions containing 2 mM

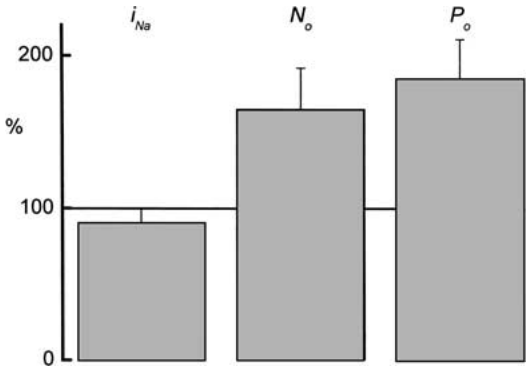

Fig. 3. Effect of Ni^{2+} on CDPC-induced noise. Noise analysis was performed by exposing the tissues alternatively to 10 and 40 μM CDPC for 5 minutes. Ni^{2+} (2 mM) drastically increased total number of channels N_o and open probability P_o and had no effect on single channel current i_{Na}.

Ni^{2+}. Ni^{2+} significantly diminished the amiloride inhibition in the range of low (< 5 μM) concentrations. At higher amiloride concentrations, the effect of Ni^{2+} is not noticeable, because the majority of Na^+ channels are blocked and the Ni^{2+} effect cannot be assessed any more. In other words, the response of Na^+ channels to Ni^{2+} is balanced by the inhibition elicited by amiloride. As the Michaelis-Menten constant (K_i) for amiloride is shifted upwards by a factor of about four, competition between Ni^{2+} (stimulating) and amiloride (blocking) seems likely. The nature of the interaction between Ni^{2+} and amiloride can be further investigated by I_{sc} fluctuation analysis of the amiloride blockade. The amiloride-induced Lorentzian components in the I_{sc} noise, which are recorded in the presence and in the absence of Ni^{2+}, show differences in corner frequencies dependent on the Ni^{2+} concentration. In Fig. 4*B* one can notice that the corner frequency decreases as the apical Ni^{2+} concentration increases. The calculation of association (k_{on}) and dissociation (k_{off}) rate constants is based on the linear fit of the $2\pi f_c$-[Ami] data. However, a large uncertainty of k_{off}, being close to zero, was found for the amiloride block (Van Driessche, 1994). The origin of the error relates to the fact that amiloride-induced noise can only be recorded with amiloride concentrations far above the Michaelis-Menten constant ($K_i = k_{off}/k_{on}$). Therefore, we can conclude at least that increased Ni^{2+} concentrations cause a decrease in amiloride k_{on}. These results may point towards a competition between Ni^{2+} and amiloride for a common binding site, although the former stimulates and the latter blocks Na^+ current.

The comparison of CDPC with amiloride gives information about the different behavior with respect to k_{on} of the two blockers. As already presented in Fig. 2, the CDPC corner frequency was not dependent on Ni^{2+}, but Fig. 4 shows this to be the case for amiloride. Clearly, the suspected Ni^{2+}-amiloride

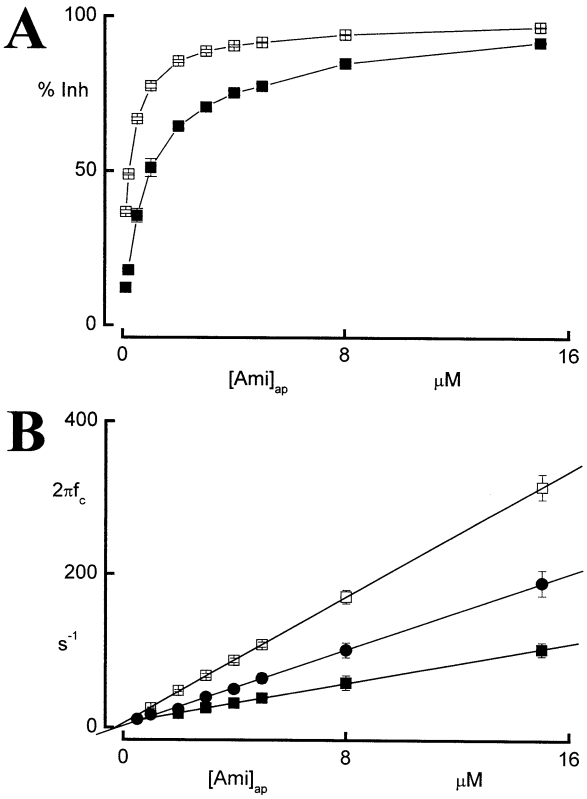

Fig. 4. Effect of Ni^{2+} on the inhibition of I_{Na} by amiloride. (*A*) Percentage inhibition of current in the absence (*white squares*) and in the presence of 2 mM Ni^{2+} (*black squares*) in the apical Ringer solution. The data are shown as the means ± SEM of 8 experiments. (*B*) Effects of Ni^{2+} on amiloride rate constants. Linear fits (solid lines) obtained by regression analysis were used to determine k_{on} and k_{off} constants of amiloride. In the absence of Ni^{2+} (*white squares*) we obtained: $k_{on} = 20.2 \pm 0.1\ \mu M^{-1}s^{-1}$, $k_{off} = 5.6 \pm 0.5\ s^{-1}$. k_{on} decreases as Ni^{2+} concentration is augmented from 0.5 (*black circles*, $k_{on} = 10.7 \pm 0.2\ \mu M^{-1}s^{-1}$, $k_{off} = 2.3 \pm 0.9\ s^{-1}$) to 2 mM Ni^{2+} (*black squares*, $k_{on} = 5.8 \pm 0.1\ \mu M^{-1}s^{-1}$, $k_{off} = 5.9 \pm 0.5\ s^{-1}$). k_{off} does not show a consistent change (*see* text).

competition has to do with the presence of the guanidinium group. In the light of these experiments we may speculate that Ni^{2+} competes with guanidinium for a common binding site, which is different from that of the pyrazine moiety.

Interactions between Ni^{2+} and Na^+

As expected from a pore blocker, amiloride interacts with Na^+. Early studies on many native epithelia demonstrated that increasing extracellular Na^+ concentrations reduced the channel affinity for amiloride. However, discrepancies exist among investigators concerning the type of amiloride inhibition. In grass frog and bullfrog skins, some authors claim a noncompetitive mechanism, while in toad and *Rana temporaria* skins the mechanism appeared to be of a mixed type competition (Benos, Mandel & Balaban,

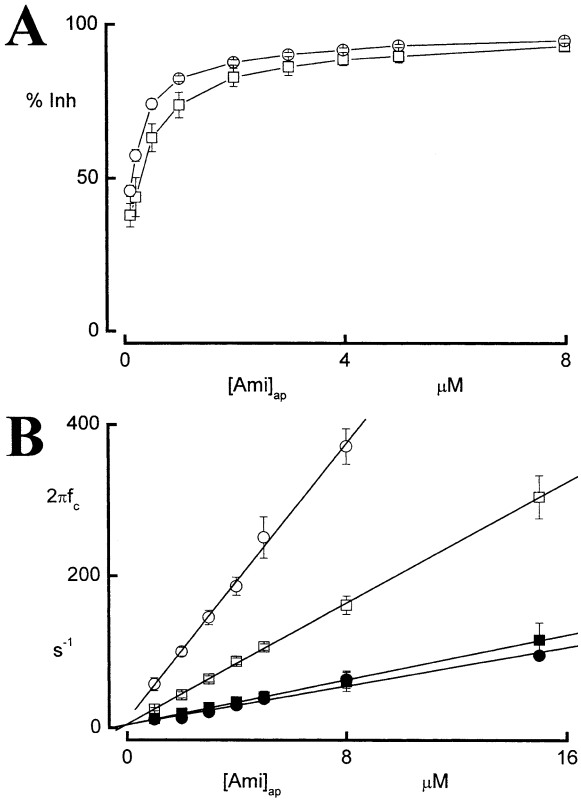

Fig. 5. Effect of increasing Na^+ concentrations on amiloride blockage. (*A*) The potency of amiloride to block I_{Na} is significantly decreased by augmenting apical Na^+ concentration from 30 (*circles*) to 102 mM (*squares*). (*B*) Amiloride noise shows a decrease in corner frequency when apical Na^+ concentration increases from 30 (*white circles*, k_{on} = 45.5 ± 1.3 $\mu M^{-1}s^{-1}$, k_{off} = 10.7 ± 5.9 s^{-1}, n = 6) to 102 mM (*white squares*, k_{on} = 19.9 ± 0.2 $\mu M^{-1}s^{-1}$, k_{off} = 4.9 ± 1.3 s^{-1}, n = 8). In the presence of 2 mM Ni^{2+} in the apical solutions f_c is much depressed and k_{on} is low and the same in 30 (*black circles*, k_{on} = 5.5 ± 0.2 $\mu M^{-1}s^{-1}$, k_{off} = 7.8 ± 1.4 s^{-1}, n = 8) and 102 mM Na^+ (*black squares*, k_{on} = 6.6 ± 0.7 $\mu M^{-1}s^{-1}$, k_{off} = 4.4 ± 0.2 s^{-1}, n = 8).

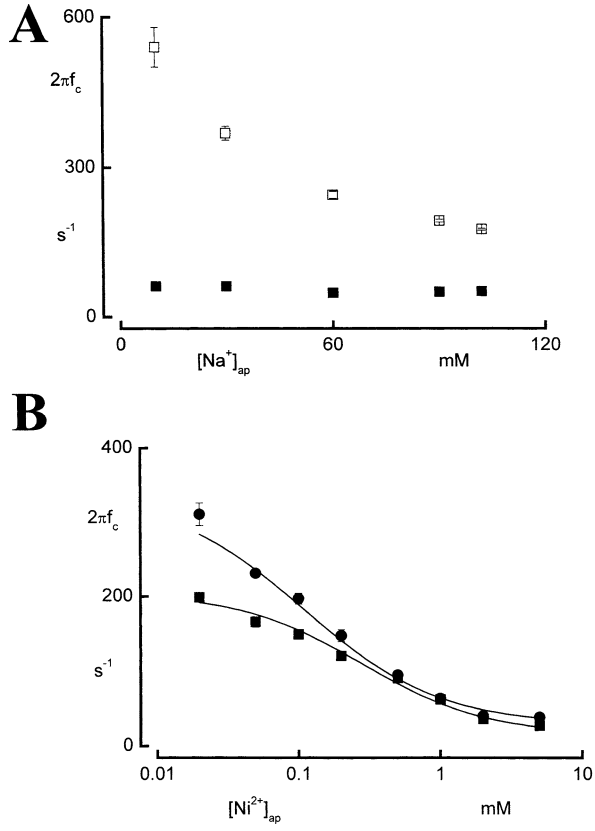

Fig. 6. Effect of Ni^{2+} concentration on Na^+-dependent amiloride noise of I_{sc}. (*A*) Dependence of f_c at 8 μM amiloride on $[Na^+]_{ap}$ (*white squares*). When 2 mM Ni^{2+} are added to the apical solutions, f_c is much suppressed and the observed decrease in f_c is abolished (*black squares*). Data are shown as averages ± SEM for 6 experiments. (*B*) Dependence of 8 μM amiloride f_c on $[Ni^{2+}]_{ap}$ in 30 (*circles*) and 102 mM $[Na^+]_{ap}$ (*squares*) in a logarithmic scale. Solid lines represent fittings with a sigmoid equation (*see* text) and the result shows that K_m values depend on Na^+ concentration.

1979). Using amiloride-induced noise analysis it had been shown that amiloride k_{on} increased as the Na^+ concentration decreased for *Rana pipiens* and *Rana temporaria* skins (Hoshiko & Van Driessche, 1986). In other words, as the Na^+ concentration decreased, blocker inhibition became more effective, i.e., Na^+ and amiloride are competitive.

In the present study, too, the I_{Na} inhibition by amiloride was diminished when apical Na^+ concentration was increased, as depicted in Fig. 5*A*. The amiloride association constant (k_{on}) diminished as well when apical Na^+ concentration was increased (Fig. 5*B*). The effect of increased Na^+ concentrations is therefore similar to the situation where addition of apical Ni^{2+} produced a k_{on} decrease for amiloride (Fig. 4*B*). It is then worthwhile to investigate a possible interaction between Na^+ and Ni^{2+}. As noise analysis gives the most accurate information about the amiloride kinetics, we performed measurements at two different Na^+ concentrations. In Fig. 5*B* we show the 2 πf_c-[Ami] relationship at 30 and 102 mM apical Na^+. The association rate constant in 30 mM $[Na^+]_{ap}$ decreased from 45.5 ± 1.3 to 5.5 ± 0.2 $\mu M^{-1}s^{-1}$ in the presence of Ni^{2+}, while in 102 mM $[Na^+]_{ap}$, k_{on} diminished from 19.9 ± 0.2 to 6.6 ± 0.7 $\mu M^{-1}s^{-1}$ when Ni^{2+} was added (n = 6). We found that in the presence of apical Ni^{2+} the on-rate constants are not statistically different in 30 and 102 mM Na^+. Moreover, we performed a more detailed amiloride-induced noise analysis at 8 μM amiloride, but varying apical Na^+. The apparent half-maximal $[Na^+]$ is around 40 mM. The decrease in f_c caused by increasing $[Na^+]_{ap}$ was completely abolished by 2 mM Ni^+ (Fig. 6*A*). In Fig. 6*B* the influence of various Ni^{2+} concentrations on f_c is shown at 30 and 102 mM apical Na^+. The data have been fitted with the following sigmoid equation:

$$y = \frac{y_1 - y_2}{1 + [Ni^{2+}]/K_m} + y_2$$

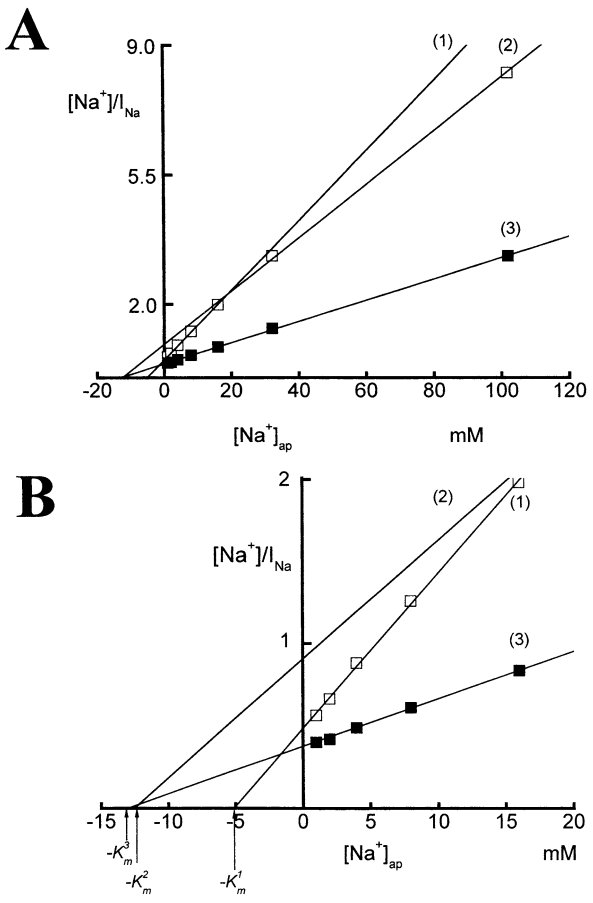

Fig. 7. Effect of $[Ni^{2+}]_{ap}$ on Na^+ kinetics. (*A*) Comparison of Hanes graphs for the kinetics of Na^+ current in control (*white squares*) and in 2 mM apical Ni^{2+} (*black squares*). In control conditions line *1* represents the linear fit for the data obtained at $[Na^+]_{ap}$ below 20 mM. The extrapolated abscissa intercept represents $-K_m^1$. Line *2* represents the linear fit for the data when $[Na^+]_{ap}$ is >20 mM and the respective intercept is $-K_m^2$. In the presence of 2 mM $[Ni^{2+}]_{ap}$ the data were fitted with a single line *3* and gave the $-K_m^3$ as abscissa intercept, almost identical to $-K_m^2$. (*B*) Magnification of plot *A* for 0–20 mM $[Na^+]_{ap}$ where the abscissa intersections of the extrapolated lines (solid lines) indicate K_m values.

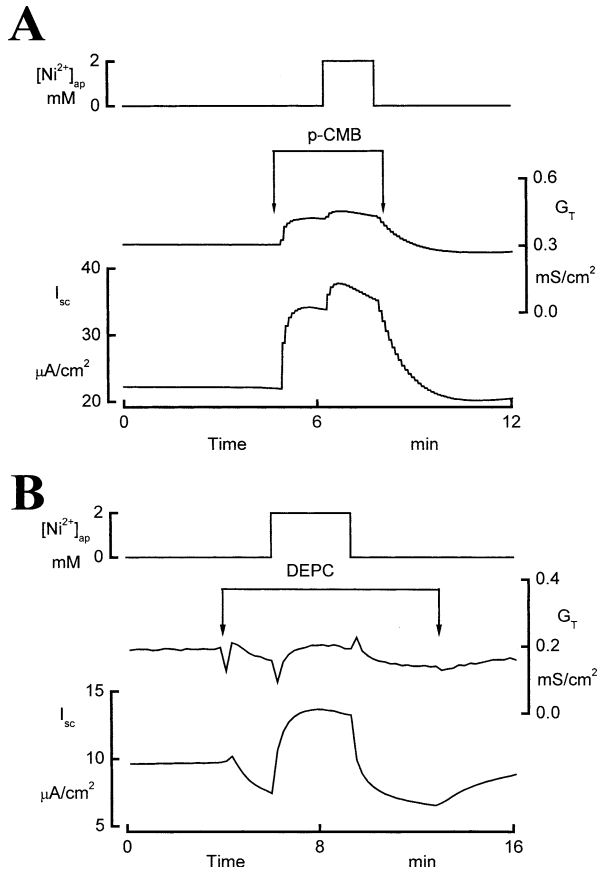

Fig. 8. Effect of $[Ni^{2+}]_{ap}$ in the presence of two putative group-specific reagents at the apical side. (*A*) The sulphhydryl blocker p-CMB (0.2 mM) causes a fast increase in current and conductance. Applied after p-CMB, Ni^{2+} has largely lost its stimulatory power. (*B*) The histidine reagent DEPC (0.5 mM) causes an inhibition of Na^+ but does preserve the stimulatory action of 2 mM Ni^{2+}.

where the fit parameters are y_1 as the initial y value, y_2 as the final y value, and K_m represents the apical Ni^{2+} concentration at which the corner frequency drops at the half-maximal value. K_m is 0.11 ± 0.01 and 0.27 ± 0.02 mM for 30 and 102 mM $[Na^+]_{ap}$, respectively. One can notice that 2 mM Ni^{2+} were sufficient to block the influence of Na^+ concentration on f_c. However, the K_m values were significantly different for the two concentrations chosen. Therefore, we can assume that Ni^{2+} competes with higher affinity than Na^+ for a common amiloride binding site.

A better understanding of this process may come from the studies of Na^+ channel kinetics in the absence of amiloride. Previous studies described a universal kinetic property of Na^+ transport where saturation of I_{Na} occurs at higher apical Na^+ concentrations (>20 mM). In some tight epithelia it has been observed that, at a rapid step increase in apical Na^+ concentration, I_{Na} increases but then declines rapidly within seconds to a steady-state level (Fuchs, Larsen & Lindemann, 1977; Scholtz & Zeiske, 1988). The process was described as the recline phenomenon and later on as "Na^+ self-inhibition" (Chraibi & Horisberger, 2002). In many amphibian epithelia, self-inhibition can be abolished by apical treatment with apparently unrelated compounds such as sulphhydryl reagents (Benos, Mandel & Simon, 1980), organic cations (Zeiske & Lindemann, 1974), or inorganic divalent cations (Scholtz & Zeiske, 1988), all shown to block the recline process. The techniqe used in such a study involves a very fast solution change at the apical border of the tissues. Although reliable for amphibian skins and bladder, the procedure is not applicable for A6 monolayers, which are more fragile and can be dislodged from the filter (their culturing substrate) during a rapid solution change. Nonetheless, self-inhibition may also show up in the absolute K_m value for the Na^+ concentration de-

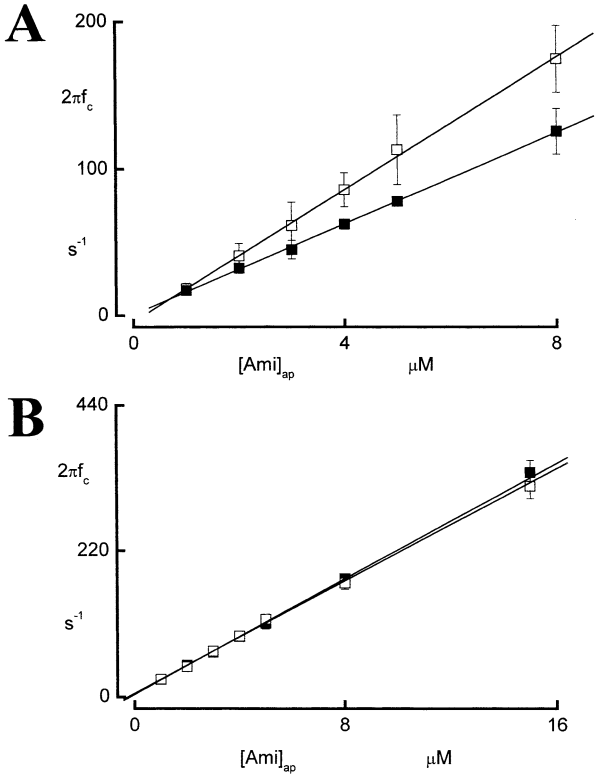

Fig. 9. Effect of Co^{2+} and Zn^{2+} on amiloride k_{on}. (*A*) Apical Co^{2+} (2 mM) causes a decrease of k_{on} from 22.9 ± 0.4 (*white squares*) to 15.8 ± 0.4 $\mu M^{-1}s^{-1}$ (*black squares*). (*B*) 0.1 mM Zn^{2+} (*black squares*) has no effect on f_c. Data are shown as averages ± SEM for 6 experiments.

pendence. A high K_m value is characteristic of a late or a lack of saturation, while a low K_m value is typical of an early saturation (Smets et al., 1998). According to Eq. 8, I_{Na} saturation may reflect saturation of i_{Na}, N_o or both. In A6 epithelial cells, previous assessment of I_{Na} kinetics yielded a K_m value of ≈5 mM, but turned out to be due to Na^+-concentration dependent changes of both i_{Na} and N_o. The process was described to reflect a saturation of i_{Na} on one hand and, on the other hand, an additional decrease of N_o as a function of $[Na^+]_{ap}$, thus resembling a recline (Smets et al., 1998). The change in N_o occurred with a very steep function between 5 and 20 mM $[Na^+]$. We decided to study Na^+ kinetics below 20 mM. In this range amphibian skin and bladder had been shown earlier (Van Driessche & Lindemann, 1979; Els & Chou, 1993) to exhibit a steep N_o drop with increasing $[Na^+]_{ap}$.

Figure 7*A* shows a Hanes plot in control and in the presence of 2 mM apical Ni^{2+} for a typical experiment in a series of four. The linear least-squares fitting resulted in a higher regression coefficient when data where fitted with two lines than with one line. The data in the interval of Na^+ concentration up to 20 mM were fitted with a first line. Its negative abscissa intercept K_m^1 determined by the extrapolation of the regression was ≈5 mM $[Na^+]_{ap}$. A second line fits the data between 20 and 102 mM $[Na^+]_{ap}$ and gives a K_m^2 around 12 mM $[Na^+]$. It is likely that K_m^1 reflects the Na^+-dependent decrease of N_o, whereas K_m^2 represents the i_{Na} saturation above this concentration, where N_o is no more dependent on $[Na^+]_{ap}$ (Smets et al., 1998). In case Ni^{2+} behaves as a blocker of Na^+ self-inhibition, N_o should remain permanently high and $[Na^+]$-independent, i.e., a recline-phenomenon (if measurable) would no longer occur. The Na^+ current is then solely determined by the i_{Na} saturation with $K_m^3 = 14$ mM $[Na^+]_{ap}$ as determined by fitting only one linear regression function to the data in the presence of Ni^{2+}. Indeed, the formerly double-linear fit becomes mono-linear, the slope is decreased (reflecting an increased maximal I_{Na}), K_m^1 becomes equal to K_m^2. Figure 7*B* represents a magnified version of the same experiment as in Fig. 7*A*, so that abscissa intercepts and the differences between K_m in control and in the presence of Ni^{2+} become evident.

Effects of Ni^{2+} in the Presence of Other Known Na^+ Transport Modifiers

The results obtained so far indicate that Ni^{2+} acts on ENaC in A6 cells by increasing only P_o, and therefore N_o (*see* Eq. 8), suggesting the release of the channel from self-inhibition. Ni^{2+} might compete for a putative binding site with the amiloride guanidinium moiety as well as with Na^+ (*see* Figs. 4 to 6). Other compounds such as the trivalent La^{3+}, organic compounds (p-CMB and benzimidazoly-2-guanidinium, BIG) or divalent cations like Ca^{2+} and Cd^{2+} were proven to abolish self-inhibition in several native epithelia (Zeiske, 1979). Although similar in their effect on Na^+ current, the binding sites for these agents may be different but, perhaps, close to each other. In order to investigate two possible binding sites for Ni^{2+}, we used two compounds: p-CMB as sulphhydryl and DEPC as a histidine reagent, which are discussed as high-affinity ligands for thiols and histidine, respectively. The mercurial compound p-CMB is known as a blocker of Na^+ self-inhibition in frog skin (Li & Lindemann, 1983), colon epithelium and mouse ENaC-expressing oocytes (Chraibi & Horisberger, 2002). The effect has been interpreted to reflect an interaction of the agent with one or more sulphhydryl groups on ENaC. In our hands, p-CMB caused a rapid and reversible transient increase of I_{sc} and G_T, followed by a decrease (*not shown*). Figure 8*A* illustrates the effect of Ni^{2+} after addition of 0.2 mM p-CMB (the maximal concentration that was soluble in Ringer solution). Like Ni^{2+}, p-CMB caused a rapid increase in current by about 54%. Added after p-CMB, the Ni^{2+}-stimulated current is only by about 10% larger than that obtained with p-CMB. These results may suggest that Ni^{2+}, as a heavy metal, and p-CMB, containing mercury, share a common bind-

ing site, e.g., one or more SH-groups. The fact that Ni^{2+} stimulation is not completely abolished by p-CMB might be due to the concentration limit reached for p-CMB or to the existence of several SH-groups that are better accessible to the smaller Ni^{2+} ions.

Studies of mouse-ENaC expressed in *Xenopus laevis* oocytes led to the assumption that histidine is a putative Ni^{2+} binding site. Like conserved cysteine regions, also a strategic histidine group was found for mouse-ENaC (Sheng et al., 2002): Ni^{2+} inhibition of ENaC was abolished after pretreatment with the histidine-modifying reagent DEPC. In our hands, DEPC caused an inhibition of the Na^+ current, while subsequent Ni^{2+} treatment still gave an enhancement of the Na^+ current by 40% (Fig. 8*B*). From these results, we may exclude, for A6 tissues, the possibility that Ni^{2+} binds to a histidine-containing site and so stimulates Na^+ current. However, putative histidine-modification by DEPC reversibly blocks I_{Na} (*see* Fig. 8*B*). This then should occur at a site different from that of stimulation by Ni^{2+}. Thus, DEPC could bind to histidine (in contrast with Ni^{2+}) and so inhibit I_{Na} as did Ni^{2+} in mouse-ENaC.

In Fig. 9 we show the results obtained with two other divalent cations on the amiloride-induced noise. Amiloride k_{on} was decreased by concentrations of Co^{2+} comparable to those of Ni^{2+} (Fig. 9*A*), but was not affected by Zn^{2+} (Fig. 9*B*). Moreover, contrary to amphibian skin (Zeiske, 1979), Zn^{2+} (just like Ni^{2+} on mouse ENaC) turned out to be an inhibitor of Na^+ transport in A6 cells up to a concentration of 1 mM. For Zn^{2+} a blocking effect was also reported in studies on rat-ENaC-expressing oocytes (Amuzescu et al., 2003).

Discussion

In this study, we show the effects of Ni^{2+} on the epithelial Na^+ channel from A6 cells. Ni^{2+} is known as a powerful blocker for low-voltage-activated Ca^{2+} channels (Perchenet, Benardeau & Ertel, 2000), while for high-voltage-activated Ca^{2+} channels it is a low-affinity blocker. Contrary to other divalent cations that can permeate Ca^{2+} channels, Ni^{2+} has the ability to bind to a regulatory site in the external part of the protein (McFarlane & Gilly, 1998). The geometric flexibility of Ni^{2+} allows formation of different complexes with amino-acid residues. Due to these special properties, Ni^{2+} is a useful tool for studies of channel gating and to probe regulatory sites in the external part of the proteins.

Mechanism of A6 ENaC Activation by Ni^{2+}

In experiments where the cells were superfused with solutions containing Ni^{2+}, current and conductance were stimulated in few seconds, the time necessary for the solution to reach the chamber. Similarly, the stimulation was reversed quickly by returning to a Ni^{2+}-free solution. The onset of activation as well as the perfect reversibility of the process suggests a site of action on the extracellular face of the channel. In addition, a covalent Ni^{2+} binding seems, therefore, unlikely. Contrary to the stimulation of I_{Na} by hormones, which cause an increase of total capacitance (Erlij et al., 1994), the enhancement of Na^+ current by Ni^{2+} is not paralleled by an increase of capacitance. This implies a stimulation of silent Na^+ channels in the apical membrane and not the insertion of new channels by exocytosis. On oocytes expressing mouse ENaC, the inhibition of Na^+ current by Ni^{2+} has been described with a maximal effect observed one minute after quick solution exchange (Sheng et al., 2002). The authors have assumed that a putative Ni^{2+} binding site is extracellularly located. In native epithelia like amphibian skin, Ni^{2+} causes stimulation of Na^+ transport, while in rat- and mouse-ENaC-expressing oocytes the effect is an inhibitory one. It cannot be excluded that Ni^{2+} effects depend on whether the channel is native or exogenously expressed. In native channels, some other proteins may be involved in the activation process. Alternatively, Ni^{2+} effects may be species-dependent.

In our study, we used for the first time CDPC-induced noise for investigation of Ni^{2+} effects on ENaC kinetics. In the presence of Ni^{2+}, we could observe a noticeable increase of N_o in the plasma membrane, which may reflect the increase of P_o. The control of the spontaneous ENaC open probability (P_o) is not completely understood. Previous experiments have shown that this channel exhibits two main conformations: one with a high P_o at low external $[Na^+]$ and one with a low P_o at high $[Na^+]_{ap}$ (Palmer & Frindt, 1996). According to this model, when the channel is exposed to Ni^{2+}, ENaC may change from the low to the high P_o mode, which is then reflected by the increase of N_o.

In A6 cells, hormones such as insulin and aldosterone cause an increase of Na^+ transport together with modification of the ENaC kinetics (Blazer-Yost et al., 1998; Erlij et al., 1994). Using the same protocol of CDPC-induced noise, the authors have shown that these hormones effect an increase in the total number of channels, without changes in P_o. These results emphasize the hypothesis that the activation of the ENaC by hormones has a pathway different from that of the stimulation by divalent cations, e.g., Ni^{2+} in A6 cells.

The effect of Ni^{2+} is likely to be the result of an interaction with the open state of the ENaC channel, since the stimulation of Na^+ current is not possible when all the channels are blocked by 10 μM amiloride. At sub-maximal amiloride concentration (100 nM) the effects of Ni^{2+} are not perturbed. Amiloride decreases the number of open channels in a dose-de-

pendent manner as suggested by noise analysis (Helman & Baxendale, 1990). However, at low doses of amiloride there are still channels in the open state that can be stabilized by Ni^{2+}, and this may cause an increase of the current. Considering the Na^+-dependent gating mode of ENaC as described, it is also possible that amiloride, being competitive with Na^+, changes the channel from the high P_o to the low P_o mode, as suggested previously by Chraibi (Chraibi & Horisberger, 2002).

Ni^{2+} Interferes with ENaC Self-inhibition

Changes in N_o, and also in P_o and i_{Na} were extensively studied with respect to the current-saturation phenomenon. Using amiloride-induced noise, Van Driessche and Lindemann (1979) found that N_o steeply decreased, whereas i_{Na} linearly increased when $[Na^+]_{ap}$ was augmented. This implied that the number of open channels decreases with increasing $[Na^+]_{ap}$. Transport saturation has been attributed to two phenomena as defined by Lindemann (1984). (i) Feedback inhibition represents the downregulation of the channel density due to an increase of intracellular $[Na^+]$. (ii) Self-inhibition downregulates the channel density by Na^+ acting on the extracellular surface of the apical membrane. In A6 cells, CDPC-induced noise revealed a two-step mechanism for the saturation process dependent on $[Na^+]_{ap}$. In the range between 0 and 20 mM external Na^+, N_o decreased steeply as a function of $[Na^+]_{ap}$, whereas above this concentration it had a constant value. However, i_{Na} saturated monotonously from 0 to 120 mM $[Na^+]_{ap}$. In our experiments, the Hanes plot could be fitted with two lines corresponding to two concentration ranges (*see* Fig. 7). As described in the Results section, this is the consequence of the current saturation behavior based on the opposite Na^+ dependence of N_o and i_{Na}, respectively. When Ni^{2+} was added, the best fit was obtained with a single line and gave a higher value for K_m. The finite slope of the Hanes graph reflects saturation behaviour of i_{Na}, which has so far not been described for amphibian skin or bladder. Besides, lines *2* (control) and *3* (in the presence of Ni^{2+}) intersect almost exactly at their ordinate intercepts. Such a clockwise turn (line *3* versus *2*) is identical to the results obtained for blockers of Na^+ self-inhibition in skin or bladder. The higher value of K_m accounts also for the release of Na^+ channel from self-inhibition.

Several decades ago it was suggested that Na^+ self-inhibition involves binding of Na^+ ions to an extracellular site (Zeiske & Lindemann, 1974; Fuchs et al., 1977). This process may cause conversion from the high P_o to the low P_o state, including possibly a large conformational change or isomerization of the channel (Chraibi & Horisberger, 2002). A specific site for Na^+ binding has not been explicitly described, only a short conserved domain termed DEG residue is presumed to be involved in the binding of extracellular proteases and in Na^+ self-inhibition (Kellenberger, Gautschi & Schild, 2002). Ni^{2+} triggers the release of ENaC from self-inhibition, a process that can take place by occupying this putative Na^+ binding site. This might be done by blocking its accessibility for Na^+ via a conformational change (allosteric competition), or by competing directly with Na^+ for the same position (isosteric competition). Contrary to Na^+, Ni^{2+} binding would then induce a conversion to the low P_o state.

Ni^{2+} Reduces Amiloride Inhibition

Amiloride K_i is increased by raising the apical Na^+ concentration. Lindemann and Voûte (1976) postulated that amiloride might bind to the same modifier site as Na^+ but with higher affinity. However, there are some indications that besides its pore-blocking effect, amiloride and some of its derivates stimulate Na^+ current and release ENaC from self-inhibition (Cuthbert & Wong, 1972; Bevevino & Lacaz-Vieira, 1982; Li & Lindemann, 1983). In our hands, amiloride did not show a stimulation of the current, even in low (nM) concentrations, where it definitively has a stimulatory effect on I_{Na} in frog skin (Zeiske, 1979). Although human ENaC showed signs of a stimulatory effect of amiloride, this effect may be masked by the high-affinity pore-blockade characteristic of amiloride (Chraibi & Horisberger, 2002). This also can be so in our case and could indicate two amiloride binding sites, one stimulatory and one inhibitory.

Nickel significantly perturbed the amiloride inhibition, as shown by the increase of macroscopic K_i, as well as of the microscopic K_i, in contrast to CDPC with which Ni^{2+} did not interact. Our results suggest a competition with the guanidinium group of the amiloride molecule, as K_i increases with Ni^{2+}. Competition between Ni^{2+} and amiloride raises one problem: while Ni^{2+} has a stimulatory effect on Na^+ current, amiloride is a blocker.

Where Does Ni^{2+} Interact with the Channel?

The amiloride-binding site has been located to the pre-M2 segments of ENaC subunits that are supposed to form the outer pore of the channel (Kellenberger & Schild, 2002). One study has indicated that the amiloride molecule interacts with the channel at two distinct sites (McNicholas & Canessa, 1997). The authors presented evidence that the guanidinium group binds to homologous sites in $\alpha\beta$ and $\alpha\gamma$ channels, while pyrazine has a different binding site. Also, experiments on frog skin have shown that CDPC and amiloride have different binding sites (Flonta et al., 1998). As CDPC is a derivative of amiloride without the guanidinium moiety, these re-

sults suggest different binding sites for pyrazine and guanidinium. However, the molecular structure for two separate binding sites has not been described so far, although some aspects, in the case of amiloride, were addressed previously (Li et al., 1985).

The geometric flexibility of Ni^{2+} in aqueous solution allows associations of the hydrated metal with several amino-acid residues (Hausinger, 1993). Recent studies have suggested a new putative binding site for amiloride situated in the extracellular domain of the rat αENaC. Analysis of an anti-amiloride antibody revealed in the CRD1 of the extracellular loop a residue pattern of six amino acids (WYRFHY), including a histidine. Ni^{2+} binds with high specificity to histidine and, thus, a histidine residue contained in the putative binding site of amiloride may be responsible for the inhibitory effect of Ni^{2+} on the mouse ENaC (Sheng et al., 2002). However, the authors claimed that there are no interactions between Ni^{2+} and amiloride inhibition. A moderate dose of DEPC caused in our experiments the inhibition of Na^+ current, as in the previous study by Sheng et al. (Sheng et al., 2002), but the stimulatory effect of Ni^{2+} in A6 cells was not suppressed. Our results suggest that the binding site for Ni^{2+} is different from the one reported in studies on rat- or mouse-ENaC-expressing oocytes, and may not contain a histidine residue. On rat and mouse ENaC Ni^{2+} causes an inhibition of Na^+ current, while on A6 cells the effect is stimulatory. There are several other reports telling that some chemical compounds have dissimilar effects on ENaC, when native tissues are compared to ENaC-expressing oocytes. For instance, BIG and novobiocin known as Na^+ uptake activators in amphibian skin (Johnston & Hoshiko, 1971; Zeiske & Lindemann, 1974) cause an inhibition of Na^+ current in oocytes expressing human-ENaC (Chraibi & Horisberger, 2002). P-CMB caused the increase of Na^+ current via the rabbit colon ENaC (Turnheim, Luger & Grasl, 1981), while in human-ENaC-expressing oocytes this compound caused inhibition of the current (Chraibi & Horisberger, 2002). These discrepancies might be related to the fact that the channel is heterologously expressed. Of course, we do not exclude the existence of different Ni^{2+} binding sites on ENaC due to species differences.

Ni^{2+} can also bind to cysteine in special square planar geometries. The sulphur of these residues can serve as a redox centre, a nucleophile, a determinant of protein tertiary structure, a Brönsted base, or a Lewis base for binding metal ions. Cysteine-metal ion binding is found in cysteine-rich metallothioneins, whose roles include scavenging excess essential metals or sequestering potentially toxic metals. All ENaCs described by molecular biology methods contain two or three cysteine rich domains (CRD). A very interesting study concerning the implication of the cysteines in the channel function was performed on the ryanodine receptor calcium release channel (RyRs) that contains 80–100 cysteine residues per subunit (Dulhunty et al., 2000). The authors have described four major classes of cysteine residues with dissimilar functional roles. By covalent modifications of these cysteines RyRs can be either activated or inhibited. A battery of free and modified thiols, with different actions on this channel, allows for a differential response. As, in ENaC channel, the number of cysteines is rather large, it is possible that not all the cysteines are involved in disulfide bonds, but some of them are free and thus susceptible for interactions especially at reducing ambient conditions. The sulphhydryl-reactive metals include very toxic metals such as mercury, cadmium and lead, but also nickel, zinc and the p-CMB reagent. P-CMB causes in A6 cells a stimulation of the Na^+ current apparently through the same pathway as Ni^{2+} does. We assume that a putative binding site for Ni^{2+} contains free cysteines from the extracellular loop of ENaC. By analogy (*see* Fig. 9), Co^{2+} ions, which are most similar to Ni^{2+}, may act in the same way. Interestingly, Zn^{2+} does not cause a stimulation of the current, but has a highly specific inhibitory effect, although it is also a sulphhydryl-reactive metal (Amuzescu B., 2003). The effect of Zn^{2+} does not alter amiloride inhibition and has a mechanism different from that of Ni^{2+} or hormones. As described for RyRs it may be that also in ENaC, Ni^{2+} and Zn^{2+} react with different cysteine groups (and probably in different ligand geometries) that have a different environment on the extracellular side. More precisely, the putative Ni^{2+} binding site, which we assume to be common to that of amiloride and Na^+, may contain other residues in addition to cysteines and thus be more specific for Ni^{2+}. Like Zn^{2+} and Cd^{2+}, which have complete 3d-electron shells, the trio of metal ions, cobalt (II), nickel (II), and copper (II), all with 3d-electron gaps, are well-known diagnostic substitutes for each other or for other essential metals in cysteine protein environments. In our experiments, too, Co^{2+} seems to bind to the same site as Ni^{2+} but with a lower affinity.

Why Nickel?

As a naked ion, Ni^{2+} can coordinate in a manifold way with nucleophiles; the resulting complexes are generally very stable and may be responsible for the effects observed here, e.g., with SH-groups. Ni^{2+} ions can coordinate up to six water molecules in aqueous solution (Hausinger, 1993). This hydration may enable interactions, e.g., hydration bonding over large molecular distances, by crossing long or several channel units (McFarlane & Gilly, 1998). For cyclic nucleotide-gated channels or for mouse ENaC, it was demonstrated that Ni^{2+} binds to several domains. Along with the geometric flexibility, these characteristics make Ni^{2+} a tool for studies of the gating

properties and ligand sites in proteins. In our studies performed on rat-ENaC-expressing oocytes and A6, respectively, Ni^{2+} shows different effects indicating different binding sites on ENaC.

Whether these binding sites depend on the channel species, on the expression system, or on the channel conformation is still an open question. To answer this question, we intend to continue these studies by similar experiments with *Xenopus laevis* ENaC expressed in *Xenopus* oocytes.

This project was supported by research grants from the 'Fonds voor wetenschappelijk onderzoek-Vlaanderen' (G.0179.99 and G.0277.03), the Interuniversity Poles of Attraction Program-Belgian State, Prime Minister's Office-Federal Office for Scientific, Technical, and Cultural Affairs IUAP P4/23. D. Cucu was supported by the Research Council scholarships program of the K.U.Leuven.

References

Aguilera, A.J., Kirk, K.L., DiBona, G.F. 1978. Effect of magnesium on sodium transport in toad urinary bladder. *Am. J. Physiol.* **234:**F192–F198

Amuzescu, B., Segal, A., Flonta, M.-L., Simaels, J., Van Driessche, W. 2003. Zinc is a voltage-dependent blocker of native and heterologously expressed epithelial Na^+ channels. *Pfluegers Arch.* **466:**69–77

Benos, D.J., Mandel, L.J., Balaban, R.S. 1979. On the mechanism of the amiloride-sodium entry site interaction in anuran skin epithelia. *J. Gen. Physiol.* **73:**307–326

Benos, D.J., Mandel, L.J., Simon, S.A. 1980. Effects of chemical group-specific reagents on sodium entry and the amiloride binding site in frog skin: evidence for separate sites. *J. Membrane Biol.* **56:**149–158

Benos, D.J., Stanton, B.A. 1999. Functional domains within the degenerin/epithelial sodium channel (Deg/ENaC) superfamily of ion channels. *J. Physiol.* **520:**631–644

Bevevino, L.H., Lacaz-Vieira, F.L. 1982. Control of sodium permeability of the outer barrier in toad skin. *J. Membrane Biol.* **66:**97–107

Blazer-Yost, B.L., Liu, X., Helman, S.I. 1998. Hormonal regulation of ENaCs: insulin and aldosterone. *Am. J. Physiol.* **274:**C1373–C1379

Chraibi, A., Horisberger, J.D. 2002. Na self inhibition of human epithelial Na channel: temperature dependence and effect of extracellular proteases. *J. Gen. Physiol.* **120:**133–145

Cuthbert, A.W., Wong, P.Y.D. 1972. The role of calcium ions in the interaction of amiloride with membrane receptors. *Molecular Pharmacol.* **8:**222–229

De Smet, P., Simaels, J., Van Driessche, W. 1995. Regulatory volume decrease in a renal distal tubular cell line (A6): I. Role of K^+ and Cl^-. *Pfluegers Arch.* **430:**936–944

De Wolf, I., Van Driessche, W. 1986. Voltage dependent Ba^{2+} block of K^+ channels in the apical membrane of frog skin. *Am. J. Physiol.* **251:**C696–C706

Denkhaus, E., Salnikow, K. 2002. Nickel essentiality, toxicity, and carcinogenicity. *Crit. Rev. Oncol. Hematol.* **42:**35–56

Dulhunty, A., Haarmann, C., Green, D., Hart, J. 2000. How many cysteine residues regulate ryanodine receptor channel activity? *Antioxid. Redox Signal* **2:**27–34

Els, W.J., Chou, K.Y. 1993. Sodium-dependent regulation of epithelial sodium channel densities in frog skin; a role for the cytoskeleton. *J. Physiol.* **462:**447–464

Erlij, D., De Smet, P., Van Driessche, W. 1994. Effect of insulin on area and Na^+ channel density of apical membrane of cultured toad kidney cells. *J. Physiol.* **481:**533–542

Flonta, M.-L., De Beir-Simaels, J., Mesotten, D., Van Driessche, W. 1998. Cu^{2+} reveals different binding sites of amiloride and CDPC on the apical Na channel of frog skin. *Biochim. Biophys. Acta.* **1370:**169–174

Fuchs, W., Larsen, E.H., Lindemann, B. 1977. Current-voltage curve of sodium channels and concentration dependence of sodium permeability in frog skin. *J. Physiol.* **267:**137–166

Garty, H., Benos, D.J. 1988. Characteristics and regulatory mechanisms of the amiloride-blockable Na^+ channel. *Physiol. Reviews* **68:**309–373

Grinstein, S., Candia, O., Erlij, D. 1978. Nonhormonal mechanisms for the regulation of transepithelial sodium transport: the roles of surface potential and cell calcium. *J. Membrane Biol.* **40:**261–280

Hausinger, R.P. 1993. Biochemistry of Nickel. Plenum Publishing Corporation, New York

Helman, S.I., Baxendale, L.M. 1990. Blocker-related changes of channel density. Analysis of a three-state model for apical Na channels of frog skin. *J. Gen. Physiol.* **95:**647–678

Hillyard, S.D., Gonick, H.C. 1976. Effects of Cd^{++} on short-circuit current across epithelial membranes. I. Interactions with Ca^{++} and vasopressin on frog skin. *J. Membrane Biol.* **26:**109–119

Hoshiko, T., Van Driessche, W. 1986. Effect of sodium on amiloride- and triamterene-induced current fluctuations in isolated frog skin. *J. Gen. Physiol.* **87:**425–442

Ismailov, I., Kieber-Emmons, T., Lin, C., Berdiev, B.K., Shlyonsky, V.G., Patton, H.K., Fuller, C.M., Worrell, R., Zuckerman, J.B., Sun, W., Eaton, D.C., Benos, D.J., Kleyman, T.R. 1997. Identification of an amiloride binding domain within the alpha-subunit of the epithelial Na^+ channel. *J. Biol. Chem.* **272:**21075–21083

Jans, D., Simaels, J., Cucu, D., Zeiske, W., Van Driessche, W. 2000. Effects of extracellular Mg^{2+} on transepithelial capacitance and Na^+ transport in A6 cells under different osmotic conditions. *Pfluegers Arch.* **439:**504–512

Johnston, K.H., Hoshiko, T. 1971. Novobiocin stimulation of frog skin current and some metabolic consequences. *Am. J. Physiol.* **220:**792–798

Kellenberger, S., Gautschi, I., Schild, L. 2002. An external site controls closing of the epithelial Na^+ channel ENaC. *J. Physiol.* **543:**413–424

Kellenberger, S., Schild, L. 2002. Epithelial sodium channel/degenerin family of ion channels: a variety of functions for a shared structure. *Physiol. Reviews* **82:**735–767

Li, J.H.Y., Cragoe, E.J., Lindemann, B. 1985. Structure-activity relationship of amiloride analogs as blockers of epithelial Na^+ channels: I. Pyrazine-ring modifications. *J. Membrane Biol.* **83:**45–56

Li, J.H.Y., Lindemann, B. 1980. The mechanism of chemical stimulation of amiloride sensitive Na channels. *Pfluegers Arch.* **384:**R7

Li, J.H.Y., Lindemann, B. 1983. Chemical stimulation of Na^+ transport through amiloride-blockable channels in frog skin epithelium. *J. Membrane Biol.* **75:**179–192

Lindemann, B. 1984. Fluctuation analysis of sodium channels in epithelia. *Ann. Rev. Physiol.* **46:**497–515

Lindemann, B., Van Driessche, W. 1977. Sodium-specific membrane channels of frog skin are pores: current fluctuations reveal high turnover. *Science* **195:**292–294

Lindemann, B., Voûte, C.L. 1976. Structure and Function of the Epidermis. Springer, Berlin

McFarlane, M.B., Gilly, W.F. 1998. State-dependent nickel block of a high-voltage-activated neuronal calcium channel. *J. Neurophysiol.* **80:**1678–1685

McNicholas, C., Canessa, C. 1997. Diversity of channels generated by different combinations of epithelial sodium channel subunits. *J. Gen. Physiol.* **109:**681–692

Palmer, L.G., Frindt, G. 1996. Gating of Na^+ channels in the rat cortical collecting tubule: effects of voltage and membrane stretch. *J. Gen. Physiol.* **107:**35–45

Perchenet, L., Benardeau, A., Ertel, E.A. 2000. Pharmacological properties of Ca(V)3.2, a low voltage-activated Ca^{2+} channel cloned from human heart. *Naunyn Schmiedebergs Arch. Pharmacol* **361:**590–599

Schild, L., Schneeberger, E., Gautschi, I., Firsov, D. 1997. Identification of amino acid residues in the alpha, beta, and gamma subunits of the epithelial sodium channel (ENaC) involved in amiloride block and ion permeation. *J. Gen. Physiol.* **109:**15–26

Scholtz, E., Zeiske, W. 1988. A novel synergistic stimulation of Na^+-transport across frog skin (*Xenopus laevis*) by external Cd^{2+}- and Ca^{2+}-ions. *Pfluegers Arch.* **413:**174–180

Segal, A., Cucu, D., Van Driessche, W., Weber, W.M. 2002. Rat ENaC expressed in *Xenopus laevis* oocytes is activated by cAMP and blocked by Ni^{2+}. *FEBS Lett.* **515:**177–183

Sheng, S., Perry, C.J., Kleyman, T.R. 2002. External nickel inhibits epithelial sodium channel by binding to histidine residues within the extracellular domains of alpha and gamma subunits and reducing channel open probability. *J. Biol. Chem.* **22:**50098–50111

Smets, I., Zeiske, W., Steels, P., Van Driessche, W. 1998. Na^+ dependence of single-channel current and channel density generate saturation of Na^+ uptake in A6 cells. *Pfluegers Arch.* **435:**604–609

Turnheim, K., Luger, A., Grasl, M. 1981. Kinetic analysis of the amiloride-sodium entry site interaction in rabbit colon. *Mol. Pharmacol.* **20:**543–550

Van Driessche, W. 1994. Noise and impedance analysis. *In:* Methods in Membrane and Transporter Research. J.A. Schafer, G. Giebisch, P. Kristensen, and H.H. Ussing, editors, pp. 27–80. R.G. Landes Company, Austin

Van Driessche, W., De Vos, R., Jans, D., Simaels, J., De Smet, P., Raskin, G. 1999. Transepithelial capacitance decrease reveals closure of lateral interspace in A6 epithelia. *Pfluegers Arch.* **437:**680–690

Van Driessche, W., Erlij, D. 1991. Cyclic AMP increases electrical capacitance of apical membrane of toad urinary bladder. *Arch. Internal. Physiol. Biochim.* **99:**409–411

Van Driessche, W., Lindemann, B. 1979. Concentration dependence of currents through single sodium-selective pores in frog skin. *Nature* **282:**519–520

Watt, R.K., Ludden, P.W. 1999. Nickel-binding proteins. *Cell. Mol. Life Sci.* **56:**604–625

Zeiske, W. 1979. Die Na^+-Aufnahme durch die apikale Membran des Froschhautepithels—ihr Mechanismus und ihre Steuerung durch Ionen und lipophile Substanzen. Universität des Saarlandes, Saarbrücken

Zeiske, W., Lindemann, B. 1974. Chemical stimulation of Na^+ current through the outer surface of frog skin epithelium. *Biochim. Biophys. Acta* **352:**323–326